Published in final edited form as:
Cell Metab. 2010 June 9; 11(6): 543–553. doi:10.1016/j.cmet.2010.04.007.

GLP-1 inhibits and adrenaline stimulates glucagon release by differential modulation of N- and L-type Ca^{2+} channel-dependent exocytosis

Yang Z De Marinis[#1], **Albert Salehi**[#1], **Caroline E Ward**[#2], **Quan Zhang**[#2], **Fernando Abdulkader**[2,5], **Martin Bengtsson**[2], **Orit Braha**[2], **Matthias Braun**[2], **Reshma Ramracheya**[2], **Stefan Amisten**[2], **Abdella M Habib**[3], **Yusuke Moritoh**[2], **Enming Zhang**[1], **Frank Reimann**[3], **Anders Rosengren**[1], **Tadao Shibasaki**[4], **Fiona Gribble**[3], **Erik Renström**[1], **Susumu Seino**[4], **Lena Eliasson**[1], and **Patrik Rorsman**[2]

[1]Lund University Diabetes Centre, Department of Clinical Sciences, Clinical Research Centre, Lund University, SE20502 Malmö, Sweden

[2]Oxford Centre for Diabetes, Endocrinology and Metabolism, University of Oxford, Churchill Hospital, Oxford OX3 7LJ, UK

[3]Cambridge Institute for Medical Research, Addenbrooke's Hospital, University of Cambridge, Cambridge CB2 0XY, UK

[4]Division of Cellular and Molecular Medicine, Department of Physiology and Cell Biology, Kobe University Graduate School of Medicine, 7-5-1 Kusunoki-cho, Chuo-ku, Kobe, Hyogo 650-0017, Japan

[5]Department of Physiology and Biophysics, Institute of Biomedical Sciences, University of São Paulo, 05508-00 São Paulo, Brazil

[#] These authors contributed equally to this work.

SUMMARY

Glucagon secretion is inhibited by glucagon-like peptide-1 (GLP-1) and stimulated by adrenaline. These opposing effects on glucagon secretion are mimicked by low (1-10 nM) and high (10 μM) concentrations of forskolin, respectively. The expression of GLP-1 receptors in α-cells is <0.2% of that in β-cells. The GLP-1-induced suppression of glucagon secretion is PKA-dependent, glucose-independent and does not involve paracrine effects mediated by insulin or somatostatin. GLP-1 is without much effect on α-cell electrical activity but selectively inhibits N-type Ca^{2+}-channels and exocytosis. Adrenaline stimulates α-cell electrical activity, increases $[Ca^{2+}]_i$, enhances L-type Ca^{2+}-channel activity and accelerates exocytosis. The stimulatory effect is partially PKA-independent and reduced in Epac2-deficient islets. We propose that GLP-1 inhibits glucagon secretion by PKA-dependent inhibition of the N-type Ca^{2+}-channels via a small increase in intracellular cAMP ($[cAMP]_i$). Adrenaline stimulates L-type Ca^{2+}-channel-dependent exocytosis by activation of the low-affinity cAMP sensor Epac2 via a large increase in $[cAMP]_i$.

Address correspondence to Dr Lena Eliasson (lena.eliasson@med.lu.se).

Europe PMC Funders Author Manuscripts

INTRODUCTION

Glucagon is the most important hyperglycaemic hormone of the body (Cryer, 2002). In both type-1 and type-2 diabetes, hyperglycaemia results from a combination of insufficient insulin secretion and oversecretion of glucagon (Dunning et al., 2005; Unger, 1985). In addition, glucagon secretion in diabetic patients also exhibits impaired counter-regulation and does not increase appropriately when blood glucose falls to dangerously low levels (Cryer, 2002).

Glucagon is secreted from α-cells in pancreatic islets. Secretion of glucagon is influenced by both intrinsic and paracrine control (exerted by factors released from neighbouring β- and δ-cells) (Gromada et al., 2007; Macdonald et al., 2007). Glucagon secretion is also under tight neuronal and hormonal control (Miki et al., 2001). Examples of agonists regulating glucagon release include GLP-1, GIP (glucose-dependent insulinotropic peptide) and adrenaline. These hormones all act via stimulation of cAMP production (Ma et al., 2005; Olsen et al., 2005). GLP-1 inhibits glucagon secretion, whereas GIP and adrenaline stimulate its release (de Heer et al., 2008; Pipeleers et al., 1985). How can compounds that share the same intracellular second messenger have opposite effects on secretion? The answer to this conundrum may provide valuable insights into the regulation of α-cell exocytosis.

Here we have compared the effects of GLP-1, adrenaline, GIP and forskolin (which all activate adenylate cyclase and stimulate cAMP production) on glucagon secretion and cAMP content. Our data suggest that the opposite effects of GLP-1 and adrenaline correlate with their different receptor densities and correspondingly different capacities to increase intracellular cAMP. This culminates in selective activation of two different cAMP-binding proteins with different affinities for cAMP, PKA and Epac2. We propose that variable activation of these two cAMP sensors mediates the opposite effects on glucagon secretion.

RESULTS

Comparison of the effects of GLP-1, GIP and adrenaline on glucagon secretion

Figure 1A compares the effects of GLP-1, GIP and adrenaline on glucagon secretion from mouse islets. GIP and adrenaline stimulated glucagon secretion 130% and 350%, respectively, whereas GLP-1 inhibited glucagon secretion by 50%. The latter effect did not correlate with any stimulation of insulin or somatostatin secretion (Fig. S1A-B).

The PKA-inhibitor 8-Br-Rp-cAMPS did not affect glucagon secretion observed in the absence of glucose but reduced the inhibitory and stimulatory effects of GLP-1 (to 15% reduction), GIP (to <20% stimulation) and adrenaline (to 150% enhancement). Thus, ~40% of the stimulatory action of adrenaline in this series of experiments was resistant to PKA inhibition (Fig. 1B).

The inhibitory effect of GLP-1 occurred over a wide range of glucose concentrations (1-20 mM, Fig. 1C) and was counteracted by adrenaline (Fig. 1D). GLP-1 remained inhibitory in the presence of the somatostatin receptor subtype-2 (SSTR2) antagonist CYN154806. In the

Europe PMC Funders Author Manuscripts

presence of CYN154806, glucagon secretion at 1 mM glucose alone was stimulated ~2-fold but GLP-1 still inhibited glucagon release by ~40% (Fig. 1E).

GIP, GLP-1 and β-adrenoreceptor densities in mouse α- and β-cells

Pure α- and β-cell fractions were obtained by FACS of dispersed islets from mice expressing YFP under the pro-glucagon promoter (Reimann et al., 2008). Mouse β-cells expressed the GLP-1 receptor gene (*Glp1r*) at high levels. The GIP receptor was also expressed at fairly high levels in β-cells (~25% of *Glp1r*) whereas the mRNAs for β_1 and β_2 adrenoreceptors (*Adrb1* and *Adrb2*) were only present at low levels (Fig. 1F). In mouse α-cells, *Glp1r* was expressed at 0.17% of that found in β-cells, whereas *Gipr* and *Adrb1* and *Adrb2* were expressed at 25- to 40-fold higher levels (Fig. 1G). The α-cell fraction consists almost exclusively of α-cells (99.98% based on the total amount of insulin, glucagon and somatostatin mRNA). Thus, the expression of Glp1r in α-cells is >8-fold higher than can be accounted for by contamination of the α-cell fraction by β-cells.

The PCR data were confirmed by immunocytochemistry. Eighty per cent of the insulin-positive β-cells co-stained with an anti-GLP-1R antibody, whereas only ~1% of the glucagon-positive α-cells contained detectable GLP-1R immunoreactivity (Figs. 1H and S1C).

The inhibitory effect of GLP-1 was abolished in the presence of the GLP-1R antagonist exendin (9-39) (Fig. 1I).

Increasing concentrations of forskolin and adrenaline exert dual effects on glucagon secretion

Low concentrations of forskolin (1-10 nM) mimicked the effect of GLP-1 and inhibited glucagon secretion by up to 60%, whereas high concentrations (0.1-10 μM) produced an adrenaline-like concentration-dependent stimulation (Fig. 2A). The inhibition produced by 1-10 nM forskolin is not due to stimulation of somatostatin secretion (Fig. S2) or insulin secretion (not shown but see (McQuaid et al., 2006))

Inhibition of PKA by 8-Br-Rp-cAMPS did not affect glucagon release evoked by 1 mM glucose alone (Fig. 2B). However, the inhibitory action of 3 nM forskolin was abolished. The stimulation evoked by 10 μM forskolin was completely resistant to PKA inhibition (conceivably because high cAMP levels antagonize the inhibitory action of 8-Br-Rp-cAMPS).

Measurements of cAMP in intact islets indicate that intra-islet cAMP concentration increases from ~2 fmol/islet under control conditions to ~10 fmol/islet in 10 nM forskolin and 50-100 fmol/islet in 1-10 μM forskolin (Fig. 2C). Parallel measurements of glucagon release revealed that inhibition was maximal when the islet cAMP content was ~10 fmol/islet and that stimulation occurred at concentrations above 50 fmol/islet.

We also determined the relationship between the adrenaline concentration and glucagon secretion. A high concentration of adrenaline (5 μM) stimulated glucagon secretion, whereas lower concentrations (50 pM-500 nM) were inhibitory (Fig. 2D).

Two different PKA isozymes have been identified: PKA type I and type II (PKAI and PKAII). PKAI is more sensitive to cAMP than PKAII because its regulatory subunit (PKA-RI) has a higher cAMP affinity than the regulatory subunit of PKAII (PKA-RII) (Cummings et al., 1996). We applied confocal microscopy to visualize the distribution of PKA-RI and PKA-RII. Both subunits were detected in α-cells (Fig. 2E-F). PKA-RII was present throughout the cells, whereas PKA-RI showed preferential near-plasma membrane localization (Fig. 2G-H).

Membrane potential-dependent effects of GLP-1, adrenaline and forskolin

Glucagon secretion shows a biphasic dependence on the extracellular K^+-concentration ($[K^+]_o$; (Gromada et al., 2004)). Fig. 3A shows the changes in membrane potential recorded from α-cells in intact islets when the $[K^+]_o$ was increased from 3.6 mM to 15 mM, 30 mM and 70 mM. Unlike β- and δ-cells, α-cells are electrically active at low (1 mM) glucose and many of the cells generated overshooting action potentials. Application of the highest $[K^+]_o$ resulted in a sustained depolarization, whereas the two lower $[K^+]_o$ resulted in weaker depolarization and reduced action potential amplitude. At 3.6 mM $[K^+]_o$, the action potentials peaked at −2±7 mV, which was reduced to −16±6 mV at 15 mM $[K^+]_o$ (n=4; $p<0.05$).

Fig. 3B compares the effects of varying $[K^+]_o$ on α-cell membrane potential and glucagon secretion. The relationship between $[K^+]_o$ and membrane potential suggests a 33±3 mV change for a 10-fold variation of $[K^+]_o$ (Fig. S3). This is less than the 60 mV expected if the membrane potential was solely determined by the K^+ permeability. Increasing $[K^+]_o$ from the normal 4.7 mM to 10-15 mM inhibits glucagon secretion by ~50% and concentrations >30 mM K^+ are required to stimulate glucagon secretion.

In the presence of 10 μM forskolin, no inhibition of glucagon secretion was produced by intermediate $[K^+]_o$ (Fig. 3B). Forskolin stimulated glucagon secretion 1.4- to 5.3-fold; the strongest stimulation was observed at an $[K^+]_o$ of 15 mM. Like forskolin, adrenaline stimulated glucagon secretion at 4.7 mM, 15 mM and 65 mM $[K^+]_o$ (Fig. 3C). Increasing $[K^+]_o$ to 15 mM inhibited glucagon secretion to the same extent as that produced by GLP-1. At this intermediate $[K^+]_o$, GLP-1 exerted no additional inhibitory effect (Fig. 3C).

These observations suggest that in the presence of forskolin or adrenaline, glucagon secretion can proceed at more negative membrane potentials than under control conditions. Perforated patch whole-cell capacitance measurements were used to compare the effects of forskolin and adrenaline on exocytosis. Under control conditions, depolarization-evoked exocytosis was small, the maximum response was observed during a depolarization to 0 mV where it averaged ~50 fF. Much larger responses were obtained in the presence of 10 μM forskolin (Fig. 3D), the maximum response was observed during a depolarization to −10 mV where it averaged ~250 fF. Importantly, exocytosis proceeded at membrane potentials in the presence of forskolin that were not associated with much exocytosis under control conditions. Thus, forskolin enhanced exocytosis elicited by a depolarization to −20 mV >10-fold; from 6±4 fF (n=5) under control conditions to 64±12 fF ($p<0.01$) after the addition of forskolin. Adrenaline (5 μM) had similar, albeit less pronounced effects (Fig. 3E);

exocytosis elicited by a depolarization to −20 mV increased from 1±2 fF (n=5) under control conditions to 13±3 fF ($p<0.01$) in the presence of adrenaline.

Involvement of Epac2 in the stimulation of exocytosis

The effects of forskolin and adrenaline on α–cell exocytosis were mimicked by intracellular application of 100 μM 8CPT-2Me-cAMP, a selective agonist of the low-affinity cAMP sensor Epac2 (Enserink et al., 2002). The maximum response was increased ~10-fold and depolarizations to voltages as negative as −20 mV evoked significant exocytotic responses (Fig. 4A-B). Under control conditions, a depolarization to −20 mV produced a capacitance increase of 2±1 fF (n=7), which increased to 19±3 fF ($p<0.001$, n=13) in the presence of 8CPT-2Me-cAMP. Isradipine (2 μM) inhibited the stimulation of exocytosis by 8CPT-2Me-cAMP by 60%, whereas exocytosis elicited by normal cAMP was inhibited by 90% (Fig. S4). The 8-CPT-2Me-cAMP-induced stimulation of exocytosis was associated with a doubling of the whole-cell Ca^{2+}-current, an effect antagonized by isradipine (Fig. 4C-D).

We further examined the role of Epac2 in the control of glucagon release by using islets from Epac2 knockout mice (Fig. 4E-F) (Shibasaki et al., 2007). Consistent with the results of Fig. 1, glucagon secretion in wildtype mouse islets was stimulated 5-fold by adrenaline and inhibited >60% in response to GLP-1 (Fig. 4E). In Epac2 knockout islets, GLP-1 remained inhibitory but the effect of adrenaline was limited to a ~2-fold stimulation of glucagon release. Thus, 80% of the stimulatory effect of adrenaline is Epac2-dependent. In both wildtype and Epac2-deficient islets the inhibitory effect of GLP-1 on glucagon secretion was strongly reduced by 8-Br-Rp-cAMPs (but the stimulatory effect of adrenaline in the wildtype was still statistically significant; $p<0.001$). Notably, the PKA-independent (8-Br-Rp-cAMPS-resistant) stimulation of glucagon secretion evoked by adrenaline was abolished in Epac2-deficient islets (Fig. 4F).

Effects of GLP-1 and adrenaline on $[Ca^{2+}]_i$ in α-cells in intact mouse islets

Many cells in intact islets exposed to 1 mM glucose exhibited spontaneous $[Ca^{2+}]_i$ oscillations (Fig. 5A). In a series conducted on 18 islets from 5 mice, 87±4 fluorescent cells were identified in the islet cross section (18700±1200 μm^2) cells. Of these, 24±2 cells (28%) were active at 1 mM glucose. Adrenaline elicited a strong response in 71% of the cells that were spontaneously active at 1 mM glucose (n=28 cells from 5 islets and 3 mice). The response to adrenaline consisted of a large $[Ca^{2+}]_i$ increase or a series of high-frequency oscillations. This suggests that the majority of cells active in 1 mM glucose are α-cells (Berts et al., 1996; Quoix et al., 2007). In 12 representative cells that responded to adrenaline, GLP-1 was without consistent effect and did not change the area under the curve divided by time (AUC/t). By contrast, adrenaline increased AUC/t to 220±51% of control ($p<0.05$).

Mouse α-cells are equipped with N- and L-type Ca^{2+}-channels (Macdonald et al., 2007). We compared the effects of the L- and N-type Ca^{2+}-channel blockers isradipine and ω-conotoxin on $[Ca^{2+}]_i$. In islets exposed to 1 mM glucose, ω-conotoxin reduced the $[Ca^{2+}]_i$ oscillation peak amplitudes by 39±11% ($p<0.02$; Fig. 5B). Subsequent addition of isradipine reduced the average peak height by a further 85±5% ($p<10^{-7}$). When isradipine was used

without the prior addition of ω-conotoxin, oscillation amplitudes were reduced by only 35±14% (p<0.001; Fig. S5A). Subsequent addition of ω-conotoxin lowered the amplitude by an additional 36±7% (p<0.05 vs isradipine alone). Addition of adrenaline in the combined presence of isradipine and ω-conotoxin evoked a transient elevation of $[Ca^{2+}]_i$, possibly reflecting the α_1-adrenoceptor-evoke response previously described in isolated mouse α-cells (Vieira et al., 2004).

Cyclic AMP causes a switch in the Ca^{2+}-channel dependence of exocytosis in α-cells from N- to L-type

Glucagon secretion elicited by low glucose alone was inhibited by the N-type Ca^{2+}-channel blocker ω-conotoxin but unaffected by the L-type Ca^{2+}-channel blocker nifedipine. In the presence of 10 μM forskolin, however, ω-conotoxin was almost without effect whereas the forskolin-induced stimulation was abolished by nifedipine (Fig. 5C).

We examined the ability of the Ca^{2+}-channel antagonists to block the effects of GLP-1, GIP and adrenaline on glucagon secretion (Fig. 5D-E). Glucagon secretion at 1 mM glucose was again strongly inhibited by ω-conotoxin and GLP-1 exerted no further inhibitory effect in the presence of this blocker. GIP and adrenaline stimulated glucagon release 1.6- and 3-fold under control conditions and they remained stimulatory in the presence of ω-conotoxin. Isradipine did not affect glucagon secretion at 1 mM glucose alone and the inhibitory effect of GLP-1 but abolished the stimulation evoked by both GIP and adrenaline (Fig. 5E).

Effects of GLP-1, ω-conotoxin, adrenaline and somatostatin on α-cell electrical activity

We recorded electrical activity from α-cells in intact mouse islets (Fig. 6). The effects of GLP-1 on α-cell electrical activity were tested in a total of six islets with no obvious and consistent effects. In three of the experiments, electrical activity was consistent enough to allow quantitative analysis. Addition of GLP-1 *transiently* (2-3 min) hyperpolarized the α-cell (the interspike membrane potential decreased from −51±1 mV to −57±1 mV; n=3; p<0.05). This hyperpolarization was associated with increased action potential amplitude in two of the three cells tested. The α-cells subsequently depolarized in continued presence of GLP-1 to −49±1 mV and the peak voltage of the action potentials averaged −1±4 mV (not significantly different from the 0.5±3 mV observed before addition of GLP-1). GLP-1 did not affect the frequency of the action potentials which averaged 4±2 Hz under control conditions and 3±1 Hz in the presence of GLP-1 (at steady-state).

We compared the effect of GLP-1 with that of ω-conotoxin (Fig. 6C). The N-type Ca^{2+}-channel blocker neither affected the interspike voltage (−48±2 mV before and after addition of ω-conotoxin, n=5) nor frequency (5±2 Hz under both conditions) but reduced the peak of the action potentials from −6±5 mV to −9±4 mV (p<0.05, paired t-test).

Adrenaline had more dramatic effects on α-cell membrane potential than GLP-1 (Fig. 6E). Application of adrenaline reversibly depolarized the α-cell from −49±2 mV to −40±2 mV (n=5; p<0.01). This was associated with a decrease in the action potential peak voltage from −8±2 mV to −20±1 mV (p<0.05). The action potential frequency was not affected (4±1 Hz under control conditions and 4±2 Hz in the presence of adrenaline) but their duration

increased 5-fold. Thus, the percentage of the time the membrane potential was above −20 mV increased from 2.1±0.8% under control conditions to 10±3.1% in the presence of adrenaline ($p<0.05$).

Somatostatin transiently abolished action potential firing (in 2 of 2 cells tested) and hyperpolarized the α-cells by 17 and 15 mV. Action potential firing then spontaneously resumed in the continued presence of somatostatin but their frequency was reduced by 50% and their amplitude increased by 10 and 19 mV (Fig. 6G). Both these effects promptly reversed upon removal of the hormone from the perfusion medium.

The effects of GLP-1 were also analyzed in isolated α-cells (Table S1). GLP-1 reduced the peak of the action potentials by 20 mV but did not affect interspike voltage and the frequency. These effects of GLP-1 were blocked by exendin (9-39).

GLP-1 inhibits N-type Ca^{2+}-channels

The findings that ω-conotoxin mimics the inhibitory effect of GLP-1 and that the incretin exerts no further inhibitory effect in the presence of the N-type Ca^{2+}-channel blocker (Fig. 5D) suggest that GLP-1 inhibits glucagon secretion by modulation of N-type Ca^{2+}-channel activity. We investigated this possibility by perforated patch whole-cell perforated patch measurements of α-cell Ca^{2+}-currents. GLP-1 inhibited the Ca^{2+}-current by ~20% during depolarizations to −10 and 0 mV (Fig. 7A-B). When applied to α-cells already exposed to GLP-1, the N-type Ca^{2+}-channel blocker produced no additional inhibition; ω-conotoxin when applied in the absence of GLP-1 reduced the Ca^{2+}-current by 17±7% (n=5; $p<0.05$; Fig S5B). The effects of GLP-1 on the N-type Ca^{2+}-channels are mediated by activation of PKA; no inhibition was observed in α-cells exposed to the PKA-inhibitor 8-Br-Rp-cAMPS (Fig. 7C-D). GLP-1 was without effect on non-N-type Ca^{2+}-currents as well as voltage-gated Na^{+}-currents (not shown).

Inhibition of N-type Ca^{2+}-channels with ω-conotoxin inhibits α-cell exocytosis (Macdonald et al., 2007). Given that GLP-1 mimics the effect of the N-type Ca^{2+}-channel blocker on the Ca^{2+}-current, it should exert an ω-conotoxin-like effect on exocytosis. We have previously observed that GLP-1 when applied to α-cells exposed to 5 mM glucose stimulates exocytosis (Ma et al., 2005). However, it is possible that the effects of glucose and GLP-1 in α-cells interact. We therefore re-examined the effect of GLP-1 at 1 mM glucose. Exocytosis was evoked by a train of ten 500-ms depolarizations from −70 mV to 0 mV (Fig. 7E). In a series of 6 experiments, exocytosis was reduced by ~60% (Fig. 7F). It was confirmed that exocytosis was stimulated by GLP-1 in the presence of 5 mM glucose (285±125 % at −10 mV; data not shown).

DISCUSSION

The ability of GLP-1 to both stimulate insulin secretion and inhibit glucagon secretion makes it unique and valuable as a diabetes therapeutic hormone. GLP-1 inhibits glucagon release without concomitant stimulation of insulin or somatostatin release and was unaffected by inclusion of the SSTR2 antagonist CYN154806 (Figs. 1 and S1). The finding that GLP-1 affects action potential firing in isolated α-cells also indicates that GLP-1 acts

directly on the α-cell and not via paracrine mechanisms. It is therefore intriguing that the expression of *Glp1r* (the GLP-1 receptor gene) was very low in α-cells (<0.2% of that in β-cells and only 1-2% of that of *Gipr, Adrb1* and *Adrb2* in α-cells; Fig. 1F-G). This low level of expression is in agreement with previous PCR and immunocytochemical data (Moens et al., 2002; Tornehave et al., 2008). We can discard the possibility that GLP-1 exerts its effect on glucagon release by activation of novel GLP-1 receptor undetected by the PCR primers and the antibody. This is suggested by the finding that the inhibitory effect of GLP-1 was abolished by the GLP-1 receptor antagonist exendin (9-39). As will be discussed below, the low α-cell GLP-1 receptor density has important functional implications and is, in fact, a prerequisite for its inhibitory action.

Cyclic AMP both inhibits and stimulates glucagon secretion: roles of PKA and Epac2

It is possible that the intracellular cAMP concentration may be approximately proportional to the number of G_s-coupled membrane receptors activated. We investigated the consequences this might have on glucagon release by exposing pancreatic islets to increasing concentrations of the adenylate cyclase activator forskolin (0.1 nM-10 μM). We found that high concentrations of forskolin (≥1 μM) mimicked the stimulatory effect of GIP and adrenaline on glucagon release, whereas low concentrations (1-10 nM) mimicked the inhibitory effect of GLP-1. Thus, GIP and adrenaline are 100- to 1000-fold more potent than GLP-1 (in agreement with the PCR data) at stimulating cAMP production when their effects are expressed as “forskolin equivalents”.

It is pertinent that the inhibitory effect of a low (3 nM) concentration of forskolin is prevented by pharmacological inhibition of PKA, whereas the stimulatory effects of 10 μM forskolin are resistant to this treatment (Fig. 3B). From this we conclude that the effects of low intracellular concentrations of cAMP are mediated by activation of PKA. As the effects of the higher concentrations of cAMP or forskolin are resistant to pharmacological inhibition of PKA it seems likely that they are mediated by activation of the low-affinity cAMP-sensor Epac2 (Shibasaki et al., 2007). Indeed, intracellular application of the Epac2 activator 8-CPT-2Me-cAMP mimics the effect of high intracellular cAMP concentration on exocytosis (Figs. 4E-F and S4).

Adrenaline exerts both inhibitory and stimulatory effects on glucagon secretion depending on receptor occupancy

The observation that adrenaline, like forskolin, exerts concentration-dependent inhibitory or stimulatory effects on glucagon secretion (Figs. 2A and D) has important physiological and pathophysiological implications. Stimulation of glucagon secretion was only observed at concentrations >1 μM and concentrations of ~5 nM were as inhibitory as GLP-1 (Fig. 2D). For comparison, the plasma concentrations of adrenaline in mice range from a basal 1 nM to 30 nM during severe stress (Grouzmann et al., 2003). Thus, circulating adrenaline is likely to inhibit rather than stimulate glucagon release. As stimulation only occurs at concentrations 1000-fold higher, it is possible that local release from intra-islet (nor-) adrenergic nerve endings mediate the stimulatory effects on glucagon secretion. The ability of electric stimulation of the splanchnic nerve to increase pancreatic glucagon secretion supports this scenario (Holst et al., 1986).

Low plasma concentrations of adrenaline may have similar inhibitory effects on glucagon secretion to GLP-1 due to a similar number of receptors being activated. Adrenaline binds to β_1 and β adrenergic receptors with K_i-values of ~10^{-6} M (Bylund et al., 2009). This means that at concentrations of 1-10 nM of adrenaline, only 0.1-1% of the receptors will be activated. As β-adrenoreceptors are expressed at levels 100-fold higher than *Glp1r*, a saturating concentration of GLP-1 (10-100 nM; K_d=0.5 nM; (Bylund et al., 2009)) would activate a similar number of receptors.

Diabetes has been reported to be associated with reduced expression of β-adrenergic receptors in the heart (Bidasee et al., 2008), endothelium (Bucci et al., 2004), liver and kidney (Xu et al., 2008). If the expression of β-receptors is also reduced in the pancreatic α-cells it is possible that the inhibitory effect of adrenaline on glucagon secretion would prevail. This would explain why impaired counter-regulation that is often seen in diabetic patients (Cryer, 2002).

Model

Based on these observations we propose the following model for the regulation of glucagon secretion (Fig. S6). The α-cell is electrically active during hypoglycemia. Voltage-gated N- and L-type Ca^{2+}-channels open during the firing of action potentials. Ca^{2+}-entry via the N-type Ca^{2+}-channels triggers exocytosis of glucagon-containing secretory vesicles. This accounts for the high rate of glucagon secretion during hypoglycemia (Fig. S6A). Although the N-type Ca^{2+}-channels only account for <20% of the whole-cell Ca^{2+}-current (Fig. S5C), application of ω-conotoxin inhibited glucagon secretion whilst only having a marginal effect on $[Ca^{2+}]_i$ and action potential firing. Inhibition of the L-type Ca^{2+}-channels (which account for 70% of the current (Macdonald et al., 2007)) was almost without inhibitory effect (Fig. 5D-F). The inhibitory effect of ω-conotoxin is as strong as that produced by the broad-spectrum Ca^{2+}-channel blocker Co^{2+} (Gromada et al., 2004). This supports the hypothesis that the glucagon granules are tightly associated with N-type Ca^{2+}-channels. Thus, the conduit of Ca^{2+}-entry is more important than overall $[Ca^{2+}]_i$ in regulating exocytosis. This may explain why there is such a weak apparent correlation between $[Ca^{2+}]_i$ and glucagon release (Fig. 5).

Postprandial release of GLP-1 inhibits glucagon secretion. GLP-1 binds to the low number of GLP-1Rs and causes a small increase in intracellular cAMP concentration that is just sufficient to activate PKA. PKA-dependent phosphorylation of N-type Ca^{2+}-channels leads to strong inhibition of their activity and a reduction in exocytosis (Fig. S6B). Inhibition of N-type Ca^{2+}-channels by PKA has not been reported previously but it is pertinent that this effect is not detectable in the presence of 8-Br-Rp-cAMPS (Fig. 7C-D). GLP-1 (like ω-conotoxin) has only a weak effect on α-cell electrical activity. The fact that the effect on α-cells in intact islets is weaker than that seen in isolated α-cells is probably a consequence of N-type Ca^{2+}-current (~20 pA) comprises a smaller fraction (~5%) of the total inward current in α-cells within intact islets (~400 pA) whereas its relative contribution is more important (30%) in isolated α-cells (~40 pA of ~130 pA).

At first glance, the transient repolarization produced by GLP-1 in α-cells resembles that produced by somatostatin (Fig. 6A, D). However, more detailed inspection counters the

argument that somatostatin mediates the inhibition of glucagon secretion. First, the repolarizing effect of GLP-1 is only transient and followed within a few minutes by a slight depolarization and reduction in action potential height. In contrast, somatostatin produced a sustained hyperpolarization and increased action potential height. Second, GLP-1 does not stimulate somatostatin secretion measured over 1-h incubations (Fig. S1B). This is consistent with the theory that any stimulation of the δ-cell by GLP-1 is transient. Third, the inhibitory effect of GLP-1 is (as already discussed above) maintained in the presence of SSTR2 antagonists.

GLP-1 and glucose both inhibit glucagon secretion by a mechanism involving reduced N-type Ca^{2+}-channel activity. We have proposed that glucose acts by closing K_{ATP}-channels. The K_{ATP}-channel activator diazoxide, which reverses the inhibitory action of glucose, does not antagonize the inhibitory effects of GLP-1 (Fig. S7A-B). This suggests that GLP-1 does not act by closure of the K_{ATP}-channels. This conclusion is supported by the absence of any sustained effect of GLP-1 on the inter-spike membrane potential (Fig. 6A). Thus, GLP-1 and glucose inhibit glucagon secretion by different mechanisms.

GLP-1 inhibits glucagon secretion by PKA-dependent modulation of the N-type Ca^{2+}-channels. Glucose, however, influences N-type Ca^{2+}-channel activity via changes in the α-cell membrane potential resulting from closure of the K_{ATP}-channels. This is supported by the finding that GLP-1 enhances the inhibitory effect of glucose whereas glucose exerts little additional inhibitory action when glucagon secretion is already suppressed by GLP-1 (Fig. 1C).

Adrenaline activates 100- to 1000-fold more G_s-coupled receptors than GLP-1 and thereby produces a larger increase in intracellular cAMP concentration (Fig. S7C). This leads to activation of PKA-RI and, in common with GLP-1, inhibits the N-type Ca^{2+}-channels. However, the large increase in cAMP also activates the low-affinity cAMP sensor Epac2. This increases Ca^{2+}-influx via the L-type Ca^{2+}-channels (Fig. 4C-D), in agreement with previous results in β-cells (Shibasaki et al., 2004). This expands the active zone of $[Ca^{2+}]_i$ capable of triggering exocytosis. Granules further away from the channels can now also undergo exocytosis. Indeed, the Ca^{2+}-sensitivity of exocytosis increases by a factor of >3.5 (determined from the slopes in Fig. S4C)

The switch from N- to L-type Ca^{2+}-channels correlates with a ~10 mV shift in the voltage dependence of exocytosis toward negative membrane potentials. This allows significant exocytosis at voltages as negative as −20 mV (Fig. 3D, E). This is significant because adrenaline depolarized the α-cell by ~10 mV and reduces the action potential peak voltage to −20 mV. If the voltage dependence of exocytosis had not changed, action potential firing in the presence of adrenaline would not produce much stimulation of glucagon release (Figs. 3 and 6). These effects of high intracellular cAMP (that affect the magnitude of the Ca^{2+}-current, the duration of the action potentials and release probability of the secretory granules) account for the stimulation of glucagon release by adrenaline. It has been suggested that adrenaline depolarize the α-cell through a store-operated mechanism (Liu et al., 2004). More work is required to establish precisely how adrenaline depolarizes the α-cell and extends the action potential duration.

Exocytosis triggered by intracellular application of the Epac2-selective agonist 8CPT-2Me-cAMP is partially resistant to the L-type Ca^{2+}-channel antagonist isradipine (Fig. 4B), whereas exocytosis elicited by standard cAMP in the electrode solution is almost entirely dependent on L-type Ca^{2+}-channels (Fig. S4). This difference may be due to the inhibition of N-type Ca^{2+} channels by PKA, which is activated by cAMP. However, 8CPT-2Me-cAMP does not activate PKA, so the isradipine-resistant component of exocytosis may be caused by Ca^{2+}-influx via N-type Ca^{2+}-channels. In addition to the activation of Epac2 and PKA-RI, adrenaline also activates PKA-RII, which requires higher cAMP levels than PKA-RI (Di Benedetto et al., 2008) and has a more cytoplasmic localization. We speculate that this promotes mobilization of secretory granules to release sites. This would account for the PKA-sensitive component of adrenaline-induced glucagon secretion that persists in the $Epac2^{-/-}$ islets (Fig. 4F).

Our estimates of the relative contribution of the PKA-dependent and -independent (Epac2-mediated) mechanisms to glucagon secretion are rather variable (compare Figs. 1A-B and 4). There are at least two explanations for this. First, the effects of β-adrenergic stimulation on intracellular cAMP content may vary leading to a variable activation of Epac2. This might account for the different magnitude of the 8-Br-Rp-cAMPS-resistant component seen in NMRI (Fig. 1) and C57Bl6J mice (Fig. 4). Second, there is a cross-talk between the PKA- and Epac2-mediated effects on exocytosis. Activation of PKA will, by affecting the rate of granule mobilization/priming (Gromada et al., 1997), influence the number of granules for Epac2 to act on. After inhibition of PKA, the size of the readily releasable pool is reduced and this limits the stimulation possible by Epac2 activation.

Conclusions

We show here that GLP-1 inhibits glucagon release by a direct effect on the pancreatic α-cell that is mediated by GLP-1 receptors. The action in part involves the same intracellular signalling pathways as those utilized by adrenaline to stimulate glucagon secretion. In general, there is a good agreement between the effects we now report in mouse islets with preliminary observations made in human islets.

We postulate that there is a direct correlation between the number of receptors and the capacity of the agonists to elevate intracellular cAMP. The divergent effects of adrenaline and GLP-1 can thus be explained by the much lower α-cell expression of the GLP-1 receptors than of the β-adrenoreceptors. Although the action of both compounds are mediated by elevation of cytoplasmic cAMP, adrenaline leads to much larger increases and thereby activates the low-affinity cAMP sensor Epac2 in addition to PKA. These results also illustrate that physiologically highly significant effects can be exerted by membrane receptors expressed at such low levels that they almost escape detection by immunocytochemistry and quantitative PCR.

SUPPLEMENTAL EXPERIMENTAL PROCEDURES

Islets and preparation of cells

Islets from NMRI mice were isolated by collagenase digestion and cultured in RPMI-1640 media (5 mM glucose) at 37°C and 5% CO_2 for 2-24 h prior to secretion or intracellular Ca^{2+} assays. For single-cell studies, islets were dispersed in a Ca^{2+}-free buffer and plated in 35-mm plastic dishes. Epac2-deficient mice were generated as previously described (Shibasaki et al., 2007). For the latter studies, normal age-matched C57Bl6J mice were used as controls (wildtype).

Hormone release

Briefly, batches of ten freshly isolated islets were pre-incubated in 1 ml of Krebs-Ringer buffer (KRB) supplemented with 1 mM glucose for 30 min followed by a 1h incubation in 1 ml of test KRB supplemented as indicated. Hormone contents were determined as described elsewhere (Heding, 1966; Panagiotidis et al., 1992; Tronier and Larsen, 1982). When extracellular KCl was increased, NaCl was correspondingly reduced to maintain iso-osmolarity. GLP-1, GIP and exendin-(9-39) were obtained from Bachem. KRB containing adrenaline was supplemented with ascorbic acid (10 μM) to prevent oxidation of the compound. BSA at a concentration of 0.1% was included in all these experiments.

The experiments were conducted over six years, in different laboratories and in different countries. To facilitate comparison between the different experimental series, glucagon secretion has been normalized to that measured under control (0 or 1 mM glucose) conditions. The latter values are given for the individual experimental series in the Figure legends.

Measurements of islet cAMP content

Freshly isolated islets were pre-incubated for 2h at 37°C in RPMI containing no glucose and supplemented with 0.05% BSA. The supernatant was discarded and the islets were incubated at 37°C for 30 min in 1 ml of KRB-BSA medium containing 1 mM glucose and 100 μM isobutyl methylxanthine (IBMX), supplemented with different forskolin concentrations. An aliquot of the supernatant was removed immediately after incubation and frozen for glucagon assay. cAMP was extracted by adding 400 μl of ice-cold sodium acetate buffer (50mM, pH 6.2) to the islets. Pellet samples were boiled for 10 min and sonicated on ice before being stored at -80°C. cAMP levels were determined by RIA (Amersham Pharmacia Biotech, Braunschweig, Germany).

Flow Cytometry of islet cells

Flow Cytometry of isolated islet cells from transgenic mice expressing the fluorescent protein Venus under the pro-glucagon promoter was performed using a Dakocytomation MoFlo cell sorter, with excitation set at 488 nm and emission monitored at 530 nm and 580 nm (Reimann et al., 2008). Cells were sorted into 1 ml of RNAlater (Ambion). Based on the mRNA-content, the Venus-positive fraction consisted exclusively of α-cells (99.98% based on glucagon, insulin and somatostatin mRNA transcripts). Corresponding Venus-negative cells were sorted in parallel into a separate tube (99.97% β-cells based on mRNA content).

RNA extraction and quantitative RT-PCR

Total RNA was purified from the purified cell fractions using RNeasy Mini kit (Qiagen) followed by DNase digestion (RQ1 DNase, Promega) and reverse transcription (SuperScript III, Invitrogen), according to the manufacturers' instructions. The resulting cDNA was subjected to 40 cycles of qquantitative real-time PCR (RotorGene 2000, Corbett Research) in 10 μl reactions containing 1X JumpStart PCR Master Mix (Sigma) and 0.2 uM primers (Gene ID; forward primer; reverse primer: Glp1r; CCAGGTTCCTTCGTGAATGT; GCAGGCTGGAGTTGTCCTTA: Gipr; AGACCAGGCCCCTACCC; TGTAATTGGCTCCCACACAA: Adrb1; GATCTGGTCATGGGATTGCT; CACACAGGGTCTCAATGCTG: Adrb2; CGACTACAAACCGTCACCAA; GTCCAGAACTCGCACCAGA. Data were normalized to the expression levels of Ribosomal protein S29 (Rps29) and hypoxanthine guanine phosphoribosyl transferase 1 (Hprt) in each sample. Data have been normalized to expression of Glp1r in β-cells (assigned as 100%).

Immunocytochemistry

GLP-1R immunoreactivity in mouse pancreases was detected using methods similar to those reported elsewhere (Braun et al., 2009) using rabbit anti-GLP-1R (LS-A-1205 and LS-A-1206, Lifespan, 1:100 and 1:750, respectively) antibodies.

PKA regulatory subunit type 1 (PKA-RI) and type 2 (PKA-RII) immunoreactivity was detected in mouse α-cells cultured overnight on glass cover slips, fixed with 4% paraformaldehyde in PBS for 1 h and permeabilized with 5% Triton X-100 overnight. The primary antibodies were mouse monoclonal anti-PKA RI (BD Biosciences, NJ, US; 1:50), goat anti-PKA RII (Upstate, Temecula, CA, US; 1:50) and guinea pig anti-glucagon (Jackson Immunoresearch Laboratories Inc, West Grove, PA, US; 1:500). Unspecific binding was blocked with 5% normal donkey serum (Jackson Immunoresearch Laboratories Inc, West Grove, PA). The secondary antibodies were anti-goat Cy5 (1:50) and anti-mouse Cy3 (1:50; both from Jackson Immunoresearch Laboratories Inc).

Intracellular Ca^{2+} measurements

Intact islets were loaded with fluo-4-AM (2.5 μM; from Invitrogen) in RPMI-1640 media (5 mM glucose) for >1h at room temperature. Islets were fixed with a wide-bore holding pipette and were continuously superfused and temperature-controlled (37 °C). The perfusion buffer contained (in mM) 139 NaCl, 4.7 KCl, 2 $NaHCO_3$, 0.5 NaH_2PO_4, 0.5 $MgSO_4$, 5 HEPES (pH 7.4 with NaOH), 2.6 $CaCl_2$, 1 glucose. GLP-1 (7-36) amide was obtained from Bachem. Laser scanning confocal microscopy was performed using an LSM 510 meta system (Zeiss). Excitation was with a 488 nm argon laser, and emitted fluorescence was collected through 500-550 nm band-pass filter. Increases in intracellular Ca^{2+} are displayed as upward deflections. Images were acquired at 1.5-2.5-s intervals. Prior to experimental recordings, islets were perfused for 10 min with the appropriate control solution. The recordings were replayed off-line and regions of interest (ROI) were selected and analyzed using the Zeiss LSM 510 software. All $[Ca^{2+}]_i$ data have been normalized to the responses in control experiments of the same duration in 1 mM glucose alone to compensate for any time-dependent decrease in fluo-4 fluorescence.

Capacitance measurements and whole-cell recordings of membrane currents and voltages

Whole-cell currents and exocytosis were recorded using an EPC-9 patch-clamp amplifier (HEKA Electronics, http://www.heka.com) and Pulse software (version 8.50). Exocytosis was monitored as changes in α-cell capacitance using the software-based lock-in function of the Pulse software. Single α-cells were identified by their small size and Na^+ current inactivation properties (Barg et al., 2000). The validity of this method was confirmed by immunostaining as previously described (Braun et al., 2008). The extracellular medium contained (in mM) 118 NaCl, 20 TEA-Cl (tetraethylammonium chloride), 5.6 KCl, 2.6 $CaCl_2$, 1.2 $MgCl_2$, 5 HEPES (pH 7.4 with NaOH) and glucose as indicated. Except for Figure 4C-D and Supplemental Fig. 5, in which the standard whole-cell configuration was used, the electrophysiological measurements were conducted using the perforated patch technique, and the pipette solution contained (in mM) 76 Cs_2SO_4, 10 NaCl, 10 KCl, 1 $MgCl_2$ and 5 HEPES (pH 7.35 with CsOH). Perforation was produced by addition of amphotericin B at a final concentration of 60 μg/ml amphotericin as previously described (Ammala et al., 1993). The standard whole-cell measurements were conducted using a pipette solution (dialyzing the cell interior) which consisted of (in mM) 125 CsOH, 125 glutamate, 10 CsCl, 10 NaCl, 1 $MgCl_2$, 5 HEPES (pH 7.15 with KOH), 3 Mg-ATP and 25 μM EGTA (measured resting free Ca^{2+}, 0.2 μM). Pulses were applied at low frequency (<0.05 Hz) to allow the exocytotic capacity to recover fully between the pulses.

Membrane potentials were recorded from α-cells in intact islets essentially as described previously (Gopel et al., 1999). The data were were analyzed using Clampfit 9 (Molecular Devices, Sunnyvale, CA). Interspike potentials were derived from Gaussian fit which was applied to all-point-histograms of the potential recording. Action potential peaks were detected using the Event Detection/Threshold Search program of Clampfit 9 (threshold level set to -20 mV). Action potential peak amplitudes were determined from a Gaussian fit to the distribution of all the events.

Statistical analysis

Data are presented as means and standard errors. Significance was examined by either the paired or unpaired *t*-test and, when appropriate, by multiple-comparisons analysis of variance (ANOVA) and post-test.

Supplementary Material

Refer to Web version on PubMed Central for supplementary material.

ACKNOWLEDGEMENTS

We thank Britt-Marie Nilsson and Anna-Maria Ramsey for excellent technical assistance. Supported by Diabetes UK, the Wellcome Trust, MRC, the EU (Eurodia and BioSim), the Swedish Research Council, the Swedish Diabetes Association, Japan Science and Technology Agency, the Pahlssons, Crafoord and Knut and Alice Wallenberg Foundations. LE and ER are Swedish Research Council senior scientists. SS is supported by CREST, FA was a recipient of a postdoctoral scholarship from Conselho Nacional de Desenvolvimento Cientifico e Tecnologico - CNPq, Brazil.

REFERENCES

Berts A, Ball A, Gylfe E, Hellman B. Suppression of Ca2+ oscillations in glucagon-producing alpha 2-cells by insulin/glucose and amino acids. Biochim Biophys Acta. 1996; 1310:212–216. [PubMed: 8611635]

Bidasee KR, Zheng H, Shao CH, Parbhu SK, Rozanski GJ, Patel KP. Exercise training initiated after the onset of diabetes preserves myocardial function: effects on expression of beta-adrenoceptors. J Appl Physiol. 2008; 105:907–914. [PubMed: 18583384]

Bucci M, Roviezzo F, Brancaleone V, Lin MI, Di Lorenzo A, Cicala C, Pinto A, Sessa WC, Farneti S, Fiorucci S, et al. Diabetic mouse angiopathy is linked to progressive sympathetic receptor deletion coupled to an enhanced caveolin-1 expression. Arterioscler Thromb Vasc Biol. 2004; 24:721–726. [PubMed: 14962949]

Bylund, DB.; Bond, RA.; Eikenburg, DC.; Hieble, JP.; Hills, R.; Minneman, KP.; Parra, S. IUPHAR-DB (IUPHAR). 2009.

Cryer PE. Hypoglycaemia: the limiting factor in the glycaemic management of Type I and Type II diabetes. Diabetologia. 2002; 45:937–948. [PubMed: 12136392]

Cummings DE, Brandon EP, Planas JV, Motamed K, Idzerda RL, McKnight GS. Genetically lean mice result from targeted disruption of the RII beta subunit of protein kinase A. Nature. 1996; 382:622–626. [PubMed: 8757131]

de Heer J, Rasmussen C, Coy DH, Holst JJ. Glucagon-like peptide-1, but not glucose-dependent insulinotropic peptide, inhibits glucagon secretion via somatostatin (receptor subtype 2) in the perfused rat pancreas. Diabetologia. 2008; 51:2263–2270. [PubMed: 18795252]

Di Benedetto G, Zoccarato A, Lissandron V, Terrin A, Li X, Houslay MD, Baillie GS, Zaccolo M. Protein kinase A type I and type II define distinct intracellular signaling compartments. Circ Res. 2008; 103:836–844. [PubMed: 18757829]

Dunning BE, Foley JE, Ahren B. Alpha cell function in health and disease: influence of glucagon-like peptide-1. Diabetologia. 2005; 48:1700–1713. [PubMed: 16132964]

Enserink JM, Christensen AE, de Rooij J, van Triest M, Schwede F, Genieser HG, Doskeland SO, Blank JL, Bos JL. A novel Epac-specific cAMP analogue demonstrates independent regulation of Rap1 and ERK. Nat Cell Biol. 2002; 4:901–906. [PubMed: 12402047]

Gromada J, Franklin I, Wollheim CB. Alpha-cells of the endocrine pancreas: 35 years of research but the enigma remains. Endocr Rev. 2007; 28:84–116. [PubMed: 17261637]

Gromada J, Ma X, Hoy M, Bokvist K, Salehi A, Berggren PO, Rorsman P. ATP-Sensitive K+ Channel-Dependent Regulation of Glucagon Release and Electrical Activity by Glucose in Wild-Type and SUR1−/− Mouse {alpha}-Cells. Diabetes. 2004; 53:S181–S189. [PubMed: 15561909]

Grouzmann E, Cavadas C, Grand D, Moratel M, Aubert JF, Brunner HR, Mazzolai L. Blood sampling methodology is crucial for precise measurement of plasma catecholamines concentrations in mice. Pflugers Arch. 2003; 447:254–258. [PubMed: 12905032]

Holst JJ, Schwartz TW, Knuhtsen S, Jensen SL, Nielsen OV. Autonomic nervous control of the endocrine secretion from the isolated, perfused pig pancreas. J Auton Nerv Syst. 1986; 17:71–84. [PubMed: 2877020]

Liu YJ, Vieira E, Gylfe E. A store-operated mechanism determines the activity of the electrically excitable glucagon-secreting pancreatic alpha-cell. Cell Calcium. 2004; 35:357–365. [PubMed: 15036952]

Ma X, Zhang Y, Gromada J, Sewing S, Berggren PO, Buschard K, Salehi A, Vikman J, Rorsman P, Eliasson L. Glucagon stimulates exocytosis in mouse and rat pancreatic alpha-cells by binding to glucagon receptors. Mol Endocrinol. 2005; 19:198–212. [PubMed: 15459251]

Macdonald PE, Marinis YZ, Ramracheya R, Salehi A, Ma X, Johnson PR, Cox R, Eliasson L, Rorsman P. A KATP Channel-Dependent Pathway within alpha Cells Regulates Glucagon Release from Both Rodent and Human Islets of Langerhans. PLoS Biol. 2007; 5:e143. [PubMed: 17503968]

McQuaid TS, Saleh MC, Joseph JW, Gyulkhandanyan A, Manning-Fox JE, MacLellan JD, Wheeler MB, Chan CB. cAMP-mediated signaling normalizes glucose-stimulated insulin secretion in

uncoupling protein-2 overexpressing beta-cells. J Endocrinol. 2006; 190:669–680. [PubMed: 17003268]

Miki T, Liss B, Minami K, Shiuchi T, Saraya A, Kashima Y, Horiuchi M, Ashcroft F, Minokoshi Y, Roeper J, et al. ATP-sensitive K+ channels in the hypothalamus are essential for the maintenance of glucose homeostasis. Nat Neurosci. 2001; 4:507–512. [PubMed: 11319559]

Moens K, Berger V, Ahn JM, Van Schravendijk C, Hruby VJ, Pipeleers D, Schuit F. Assessment of the role of interstitial glucagon in the acute glucose secretory responsiveness of in situ pancreatic beta-cells. Diabetes. 2002; 51:669–675. [PubMed: 11872665]

Olsen HL, Theander S, Bokvist K, Buschard K, Wollheim CB, Gromada J. Glucose stimulates glucagon release in single rat alpha-cells by mechanisms that mirror the stimulus-secretion coupling in beta-cells. Endocrinology. 2005; 146:4861–4870. [PubMed: 16081632]

Pipeleers DG, Schuit FC, Van Schravendijk CF, Van de Winkel M. Interplay of nutrients and hormones in the regulation of glucagon release. Endocrinology. 1985; 117:817–823. [PubMed: 2862020]

Quoix N, Cheng-Xue R, Guiot Y, Herrera PL, Henquin JC, Gilon P. The GluCre-ROSA26EYFP mouse: a new model for easy identification of living pancreatic alpha-cells. FEBS Lett. 2007; 581:4235–4240. [PubMed: 17706201]

Reimann F, Habib AM, Tolhurst G, Parker HE, Rogers GJ, Gribble FM. Glucose sensing in L cells: a primary cell study. Cell Metab. 2008; 8:532–539. [PubMed: 19041768]

Shibasaki T, Sunaga Y, Fujimoto K, Kashima Y, Seino S. Interaction of ATP sensor, cAMP sensor, Ca2+ sensor, and voltage-dependent Ca2+ channel in insulin granule exocytosis. J Biol Chem. 2004; 279:7956–7961. [PubMed: 14660679]

Shibasaki T, Takahashi H, Miki T, Sunaga Y, Matsumura K, Yamanaka M, Zhang C, Tamamoto A, Satoh T, Miyazaki JI, et al. Essential role of Epac2/Rap1 signaling in regulation of insulin granule dynamics by cAMP. Proc Natl Acad Sci U S A. 2007

Tornehave D, Kristensen P, Romer J, Knudsen LB, Heller RS. Expression of the GLP-1 receptor in mouse, rat, and human pancreas. J Histochem Cytochem. 2008; 56:841–851. [PubMed: 18541709]

Unger RH. Glucagon physiology and pathophysiology in the light of new advances. Diabetologia. 1985; 28:574–578. [PubMed: 3902546]

Vieira E, Liu YJ, Gylfe E. Involvement of alpha1 and beta-adrenoceptors in adrenaline stimulation of the glucagon-secreting mouse alpha-cell. Naunyn Schmiedebergs Arch Pharmacol. 2004; 369:179–183. [PubMed: 14727006]

Xu C, Arinze IJ, Johnson J, Tuy TT, Bone F, Ernsberger P, Massillon D. Metabolic dysregulation in the SHROB rat reflects abnormal expression of transcription factors and enzymes that regulate carbohydrate metabolism. J Nutr Biochem. 2008; 19:305–312. [PubMed: 17683927]

SUPPLEMENTAL REFERENCES

Ammala C, Eliasson L, Bokvist K, Larsson O, Ashcroft FM, Rorsman P. Exocytosis elicited by action potentials and voltage-clamp calcium currents in individual mouse pancreatic B-cells. J Physiol. 1993; 472:665–688. [PubMed: 8145165]

Barg S, Galvanovskis J, Gopel SO, Rorsman P, Eliasson L. Tight coupling between electrical activity and exocytosis in mouse glucagon-secreting alpha-cells. Diabetes. 2000; 49:1500–1510. [PubMed: 10969834]

Braun M, Ramracheya R, Amisten S, Bengtsson M, Moritoh Y, Zhang Q, Johnson PR, Rorsman P. Somatostatin release, electrical activity, membrane currents and exocytosis in human pancreatic delta cells. Diabetologia. 2009

Braun M, Ramracheya R, Bengtsson M, Zhang Q, Karanauskaite J, Partridge C, Johnson PR, Rorsman P. Voltage-gated ion channels in human pancreatic {beta}-cells Electrophysiological characterization and role in insulin secretion. Diabetes. 2008

Gopel S, Kanno T, Barg S, Galvanovskis J, Rorsman P. Voltage-gated and resting membrane currents recorded from B-cells in intact mouse pancreatic islets. J Physiol. 1999; 521(Pt 3):717–728. [PubMed: 10601501]

Heding, LA. A simplified insulin radioimmunoassay method; Paper presented at: Labelled proteins in tracer studies; Brussels, Euratom. 1966;

Panagiotidis G, Salehi AA, Westermark P, Lundquist I. Homologous islet amyloid polypeptide: effects on plasma levels of glucagon, insulin and glucose in the mouse. Diabetes Res Clin Pract. 1992; 18:167–171. [PubMed: 1337737]

Reimann F, Habib AM, Tolhurst G, Parker HE, Rogers GJ, Gribble FM. Glucose sensing in L cells: a primary cell study. Cell Metab. 2008; 8:532–539. [PubMed: 19041768]

Shibasaki T, Takahashi H, Miki T, Sunaga Y, Matsumura K, Yamanaka M, Zhang C, Tamamoto A, Satoh T, Miyazaki JI, Seino S. Essential role of Epac2/Rap1 signaling in regulation of insulin granule dynamics by cAMP. Proc Natl Acad Sci U S A. 2007

Tronier B, Larsen UD. Somatostatin-like immunoreactivity in man. Measurement in peripheral plasma. Diabete Metab. 1982; 8:35–40. [PubMed: 6124467]

Europe PMC Funders Author Manuscripts

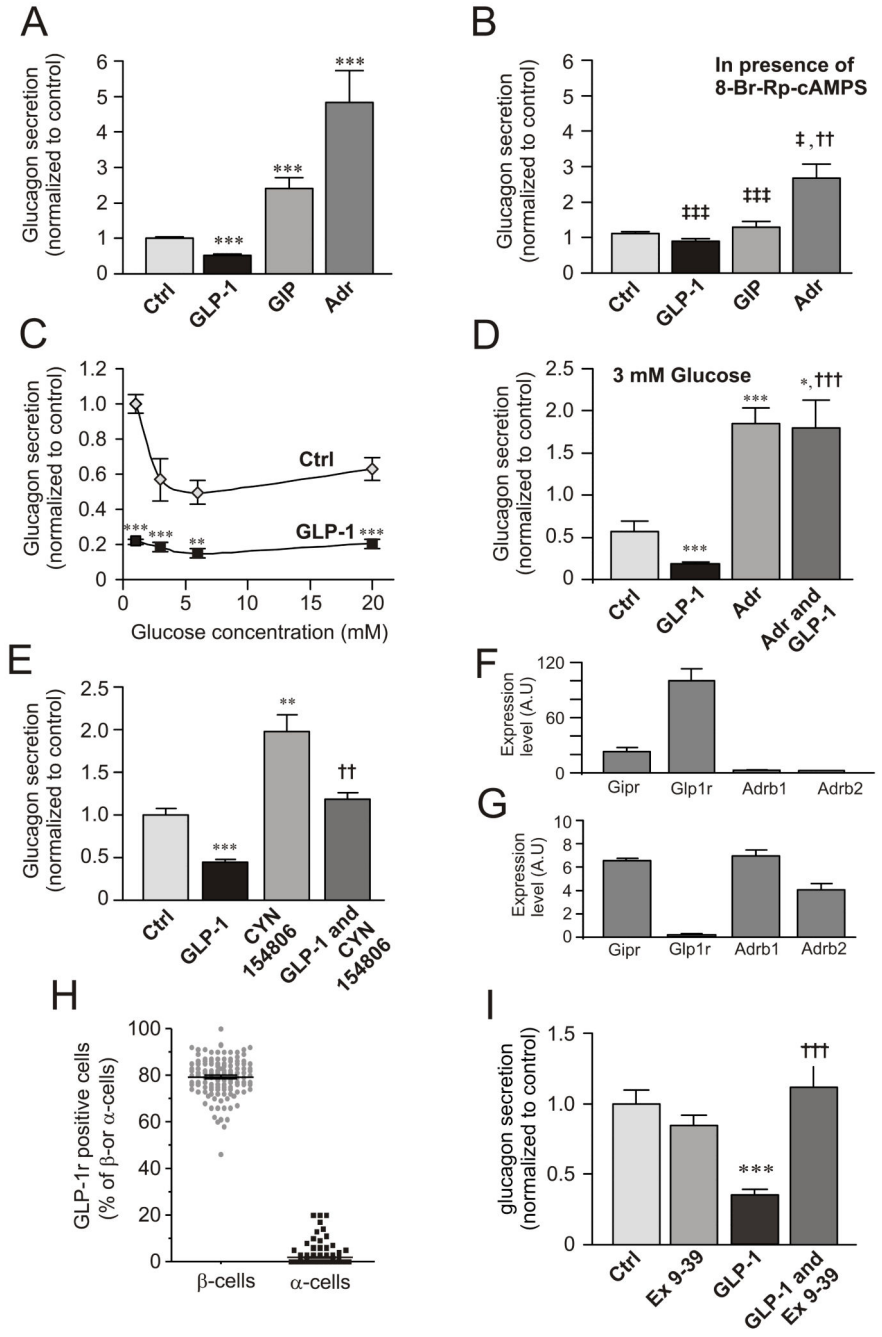

Figure 1.

Divergent effects of cAMP-increasing agents on glucagon secretion and involvement of PKA.

(A) Glucagon secretion measured from isolated mouse islets in 0 mM glucose (Ctrl) and in the presence of 100 nM GLP-1, 100 nM GIP or 5 μM adrenaline (Adr). ***p<0.001 *vs.* ctrl; (B) As in A, but in the presence of 10 μM of the PKA-inhibitor 8-Br-Rp-cAMPS as indicated. ††p<0.01 vs. Ctrl; ‡p<0.05, ‡‡‡p<0.001 for comparison with corresponding values in A. Data have been normalized to control (10.4±0.5 pg/islet/h; n=8-16).

(C) Glucagon secretion measured in the absence (◇) and presence (■) of 100 nM GLP-1 at different glucose concentrations (1-20 mM). **p<0.01 and ***p<0.001 for effect of GLP-1 compared at the respective glucose concentrations. Data have been normalized to control (1 mM glucose; 30.4±1.5 pg/islet/h; n=8).

(D) Glucagon secretion measured at 3 mM glucose in the absence and presence of 100 nM GLP-1 with or without addition of adrenaline (Adr, 5 μM). Data have been normalized to value at 1 mM (in C; 30.4±1.5 pg/islet/h; n=8). *p<0.05, ***p<0.001 vs control and †††p<0.001 vs. GLP-1.

(E) Effects of 10 nM GLP-1 in the absence and presence of 100 nM of the SSTR2 antagonist CYN154806 as indicated. Glucose was presented at 1 mM. Data have been normalized to control (2.1±0.1 pg/islet/h, n=7). **p<0.01 and ***p<0.001 vs control and ††p<0.01 vs. CYN154806 alone.

(F) Expression of GLP-1 (*Glp1r*), GIP (*Gipr*) and β1 and β2-adrenergic receptors (*Adrb1* and *Adrb2*) in mouse β-cells.

(G) Same as in F but using mouse α-cells. Data have been normalized to Glp1r expression in mouse β-cells. Note use of different ordinate scales in F-G.

(H) Fraction GLP-1R-positive cells of insulin- (β-cells) and glucagon-positive (α-cells).

(I) Glucagon secretion at 1 mM glucose (Ctrl) and in the presence of 1 μM of exendin-(9-39) (Ex 9-39) and/or 100 nM GLP-1 as indicated. Data have been normalized to control (9.3±0.3 pg/islet/h; n=11-12). ***p<0.001 *vs* control; †††p<0.001 *vs* GLP-1 alone.

Europe PMC Funders Author Manuscripts

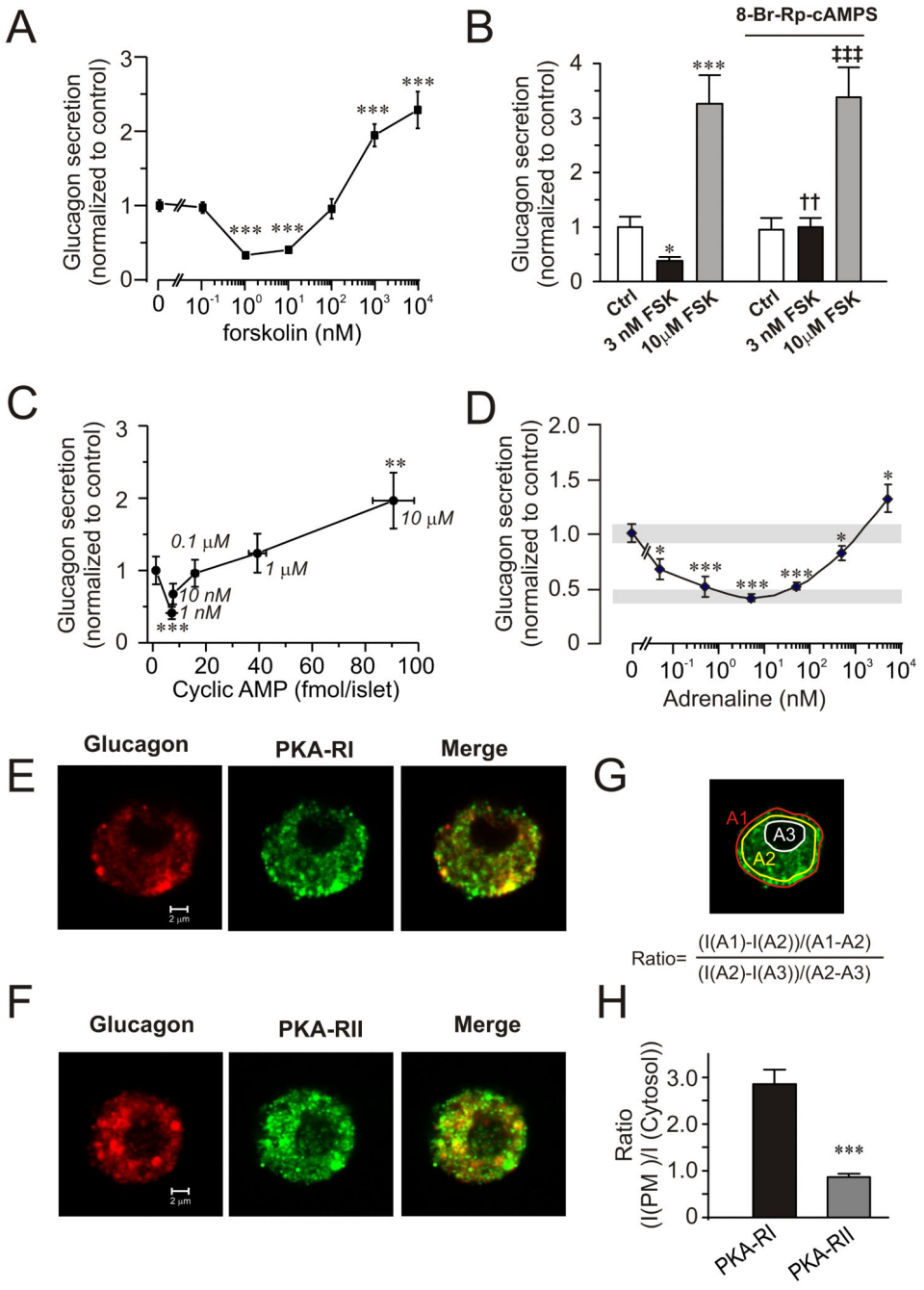

Figure 2.

Concentration-dependent effects of forskolin and adrenaline on glucagon secretion and cAMP production.

(A) Effects of increasing concentrations of forskolin (0-10 μM) on glucagon secretion at 0 mM glucose. Data have been normalized to control (13.0±0.9 pg/islet/h; n=8). ***p<0.001 *vs*. rate of secretion in the absence of forskolin.

(B) Glucagon secretion at 1 mM glucose (Ctrl) with or without addition of 3 nM or 10 μM forskolin (FSK) in the absence (left) and presence (right) of 10 μM 8-Br-Rp-cAMPS. Data

have been normalized to control (7.1±0.3 pg/islet/h; n=6-12).*p<0.05 and ***p<0.001 *vs*. Ctrl; ††p<0.01 and ‡‡‡p<0.001 *vs* Ctrl in the presence of 8-Br-Rp-cAMPS.

(C) Glucagon secretion with increasing concentrations of cAMP. Glucagon and cAMP content were measured in islets exposed to increasing concentrations of forskolin (0-10 μM; concentrations (in μM) are given next to the data points) in the presence of 1 mM glucose. Data have been normalized to control (2.8±0.5 pg/islet/h; n=8). ***p<0.001 and **p<0.01 *vs*. secretion in the absence of forskolin.

(D) Effects of increasing concentrations of adrenaline (5 pM-5 μM) on glucagon secretion. Grey rectangles indicate glucagon secretion at 1 mM glucose alone (top) and 8 mM glucose (bottom). Experiments were performed in the presence of 1 mM glucose. Data have been normalized to control (4.9±0.34 pg/islet/h; n=4). ***p<0.001 and *p<0.05 *vs.* secretion in the absence of adrenaline.

(E) Confocal immunostaining of cells dispersed from single mouse islets. Cells were labelled with antibodies against glucagon (red) and PKA-RI (green). Rightmost panel shows the superimposed images (merge).

(F) As in E but using antibody against PKA-RII.

(G) Schematic illustration of image analysis. The ratio between near-plasma membrane and cytosolic immunoreactivity was determined using the equation inserted into the image.

(H) Ratio between near-plasma membrane and cytosolic immunoreactivity calculated as illustrated in G. ***p<0.001 (n=10 for PKA-RI and PKA-RII.

Europe PMC Funders Author Manuscripts

Europe PMC Funders Author Manuscripts

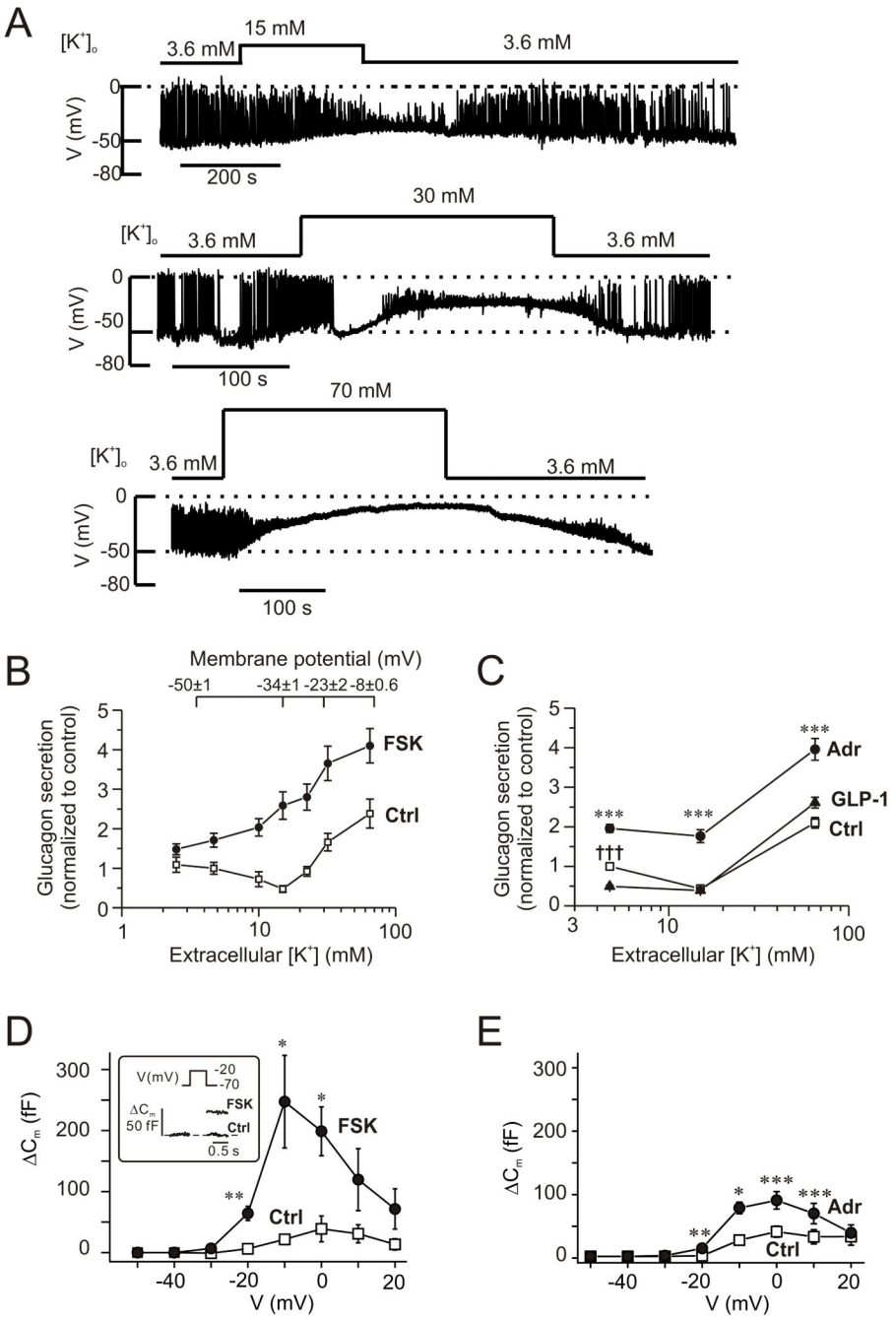

Figure 3.

Cyclic AMP-dependent modulation of the membrane potential dependence of glucagon secretion.

(A) Membrane potential recordings from α-cells within intact islets (spontaneously active at 1 mM glucose) at 3.6 mM, 15 mM, 30 mM and 70 mM extracellular K^+ (as indicated).

(B) Glucagon secretion measured at extracellular K^+ concentrations ($[K^+]_o$) between 2.5 and 65 mM under control conditions (□) and in the presence of 10 μM forskolin (●). Glucose was present at 1 mM. The membrane potentials indicated (top) were obtained from

experiments of the type as shown in A (n=7, 4, 4, 3 at 3.6 mM, 15 mM, 30 mM and 70 mM). Secretion data have been normalized to control (34.4±4.5 pg/islet/h measured at 4.7 mM $[K^+]_{o;}$ n=4-8). All values in the presence of forskolin are significantly different from corresponding control values ($p<0.01$ or better). Glucagon release under control conditions at 15 mM $[K^+]_o$ is significantly ($p<0.05$) lower, while glucagon secretion at 32 and 65 mM $[K^+]_o$ is significantly ($p<0.001$) higher than that at 4.7 mM $[K^+]_o$.

(C) Glucagon secretion measured at 4.7 mM, 15 mM and 65 mM $[K^+]_o$ (control, □) and in the presence of 5 μM adrenaline (●) or 100 nM GLP-1 (▲). Glucose was present at 1 mM. Data have been normalized to glucagon secretion at 4.7 mM $[K^+]_o$ (33.4±1.5 pg/islet/h; n=10). ***$p<0.001$ for adrenaline *vs*. control and †††$p<0.001$ for GLP-1 *vs*. control.

(D) Changes in membrane capacitance (ΔC_m) displayed against membrane potential of depolarization (V) under control conditions (□) and 4 min after application of 10 μM forskolin (●). n=5 cells. *$p<0.05$; **$p<0.01$ *vs.* control. The inset shows the response to a depolarization to −20 mV.

(E) As in D but comparing responses in the presence of 5 μM adrenaline (●) with control responses (□). n=5 cells. *$p<0.05$; **$p<0.01$; ***$p<0.001$ *vs.* control.

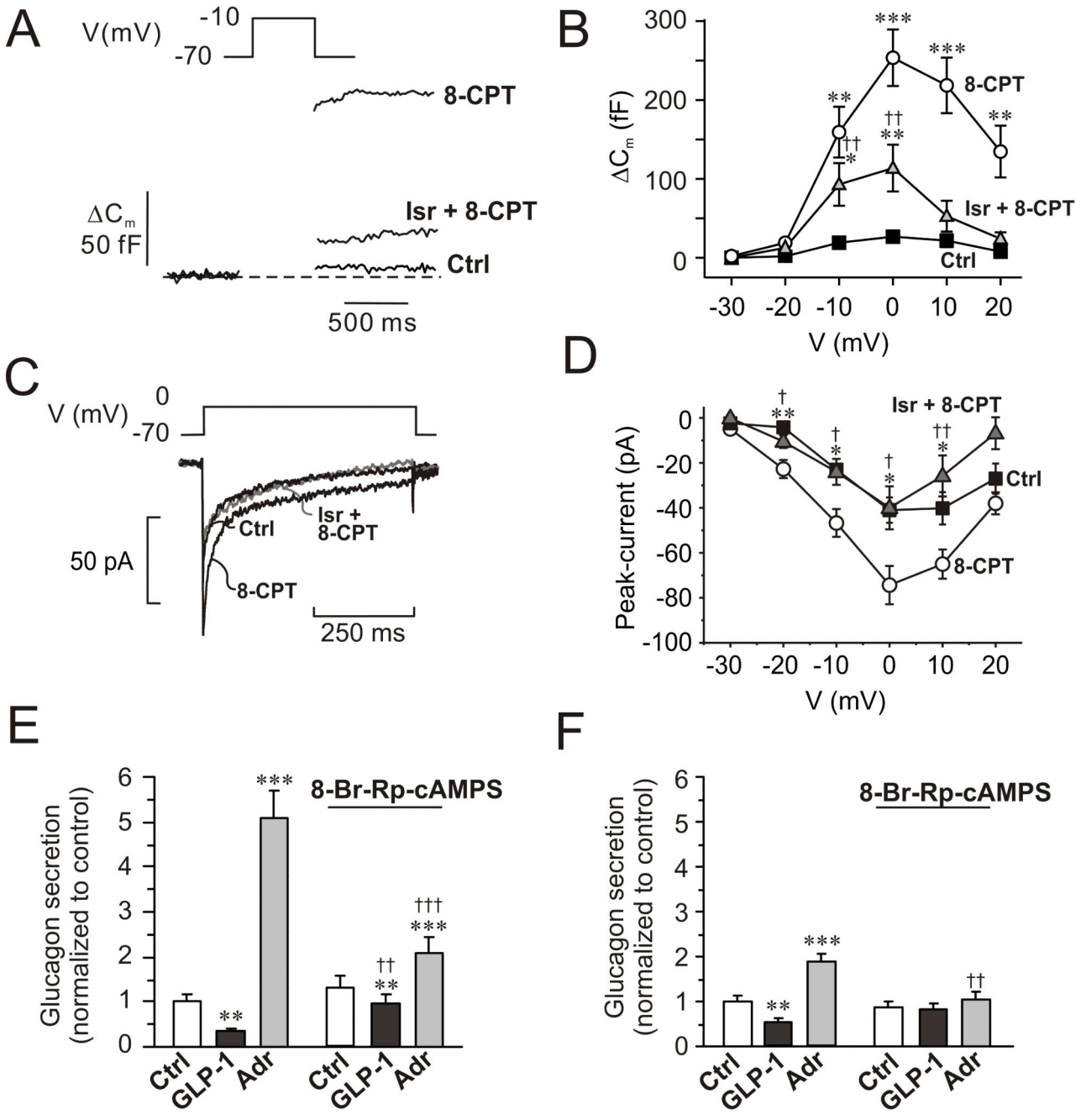

Figure 4.

Involvement of Epac2 in α-cell exocytosis and glucagon secretion.

(A) Changes in membrane capacitance (ΔC_m) elicited by voltage-clamp depolarization from −70 mV to −10 mV under control conditions (Ctrl), in the presence of 0.1 mM of the Epac2 agonist 8CPT-2Me-cAMP (8-CPT) and in the simultaneous presence of 8CPT-2Me-cAMP and 2 μM isradipine (Isr + 8-CPT).

(B) Changes in membrane capacitance (ΔC_m) displayed against membrane potential of depolarization (V) under control conditions (■), after inclusion of 0.1 mM 8CPT-2Me-

cAMP in the intracellular medium (○), and in 8CPT-2Me-cAMP containing cells exposed to 2 μM isradipine (▲). Data are mean values ± S.E.M. of 7-13 experiments. *p<0.05, **p<0.01 and ***p<0.001 for comparisons between 8CPT-2Me-cAMP alone or 8CPT-2Me-cAMP in the simultaneous presence of isradipine *vs.* control. ††p<0.01 for values in simultaneous presence of 8CPT-2Me-cAMP and isradipine *vs*. 8CPT-2Me-cAMP alone.

(C) Whole-cell Ca^{2+}-currents recorded under control conditions (Ctrl), after intracellular application of 100 μM 8-CPT-2Me-cAMP (8-CPT) and in the presence of 8-CPT and 2 μM isradipine.

(D) Peak Ca^{2+}-currents recorded under control conditions (■), after intracellular addition of 8-CPT (○) and after intracellular application of 8-CPT when L-type Ca^{2+}-channels were blocked by isradipine (2 μM). *p<0.05 and **p<0.01 for the stimulatory effects of 8-CPT (vs. Ctrl) and †p<0.05 and ††p<0.01 for the effect of isradipine (vs. 8-CPT). (n=5-10 experiments in each group)

(E) Glucagon secretion from wildtype mouse islets under control conditions (Ctrl; 1 mM glucose), in the presence of 100 nM GLP-1 or 5 μM adrenaline (Adr) in the absence and presence of 10 μM 8-Br-Rp-cAMPS. n=6-8. **p<0.01 and ***p<0.001 *vs.* Ctrl in the absence or presence of 8-Br-Rp-cAMPS; ††p<0.01 and †††p<0.001 *vs*. corresponding value in the absence of 8-Br-Rp-cAMPS. Glucose was present at 1 mM.

(F) As in C using islets from Epac2 null mice. n=5-8. **p<0.01 and ***p<0.001 *vs*. Ctrl in the absence or presence of 8-Br-Rp-cAMPS. ††p<0.05 *vs*. corresponding value in the absence of 8-Br-Rp-cAMPS.

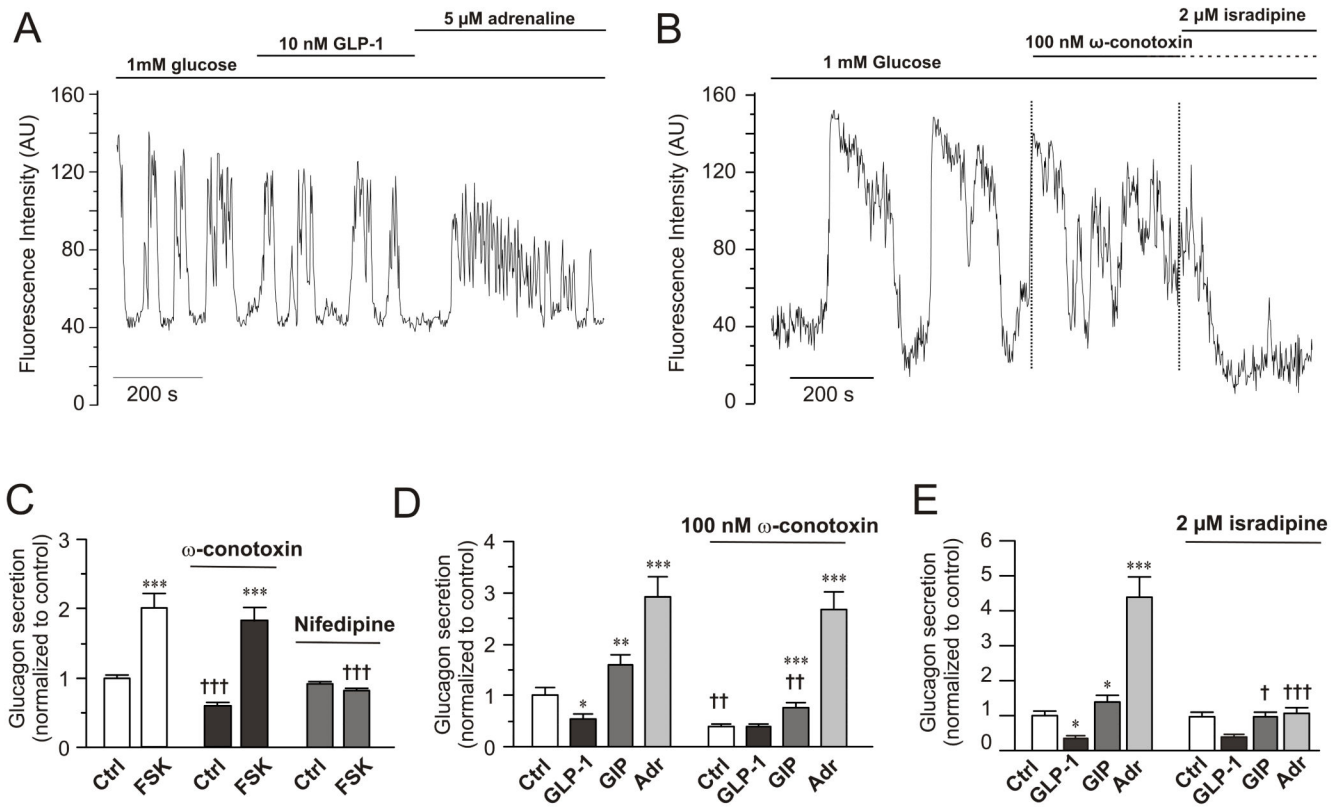

Figure 5.

Effects of GLP-1, adrenaline and Ca^{2+}-channel blockers on α-cell $[Ca^{2+}]_i$ and glucagon secretion

(A) Spontaneous $[Ca^{2+}]_i$-oscillations in individual α-cells in intact mouse islets exposed to 1 mM glucose and effects of including 10 nM GLP-1 or 5 μM adrenaline in the perfusion medium during the periods indicated by horizontal lines. n=12 cells in 4 islets from 3 mice.

(B) As in A but 100 nM ω-conotoxin and 2 μM isradipine were applied. n= 14 cells in 4 islets from 2 mice.

(C) Glucagon secretion at 1 mM glucose (Ctrl) and in the presence of 10 μM forskolin in the absence (left) and presence of 1 μM ω-conotoxin (middle) or 50 μM nifedipine (right). Data have been normalized to control in the absence of forskolin and the Ca^{2+}-channel blockers (30.7±1.2 pg/islet/h; n=8-10). ***p<0.001 *vs.* respective control (Ctrl) in the absence or presence of ω-conotoxin or isradipine. †††p<0.001 *vs.* corresponding value in the absence of ω-conotoxin or isradipine.

(D) As in C but comparing the effects of 100 nM GLP-1, 100 nM GIP and 5 μM adrenaline (Adr) in the absence (left) and presence (right) of 100 nM ω-conotoxin. n=10. *p<0.05, **p<0.01 and ***p<0.001 *vs.* respective Ctrl in the absence or presence of ω-conotoxin; ††p<0.01 *vs.* corresponding value in the absence of ω-conotoxin.

(E) As in D but 2 μM isradipine was applied. n=7-10. *p<0.05 and ***p<0.001 *vs.* Ctrl; †p<0.001 *vs.* GIP in absence of isradipine and †††p<0.001 *vs.* adrenaline in absence of isradipine.

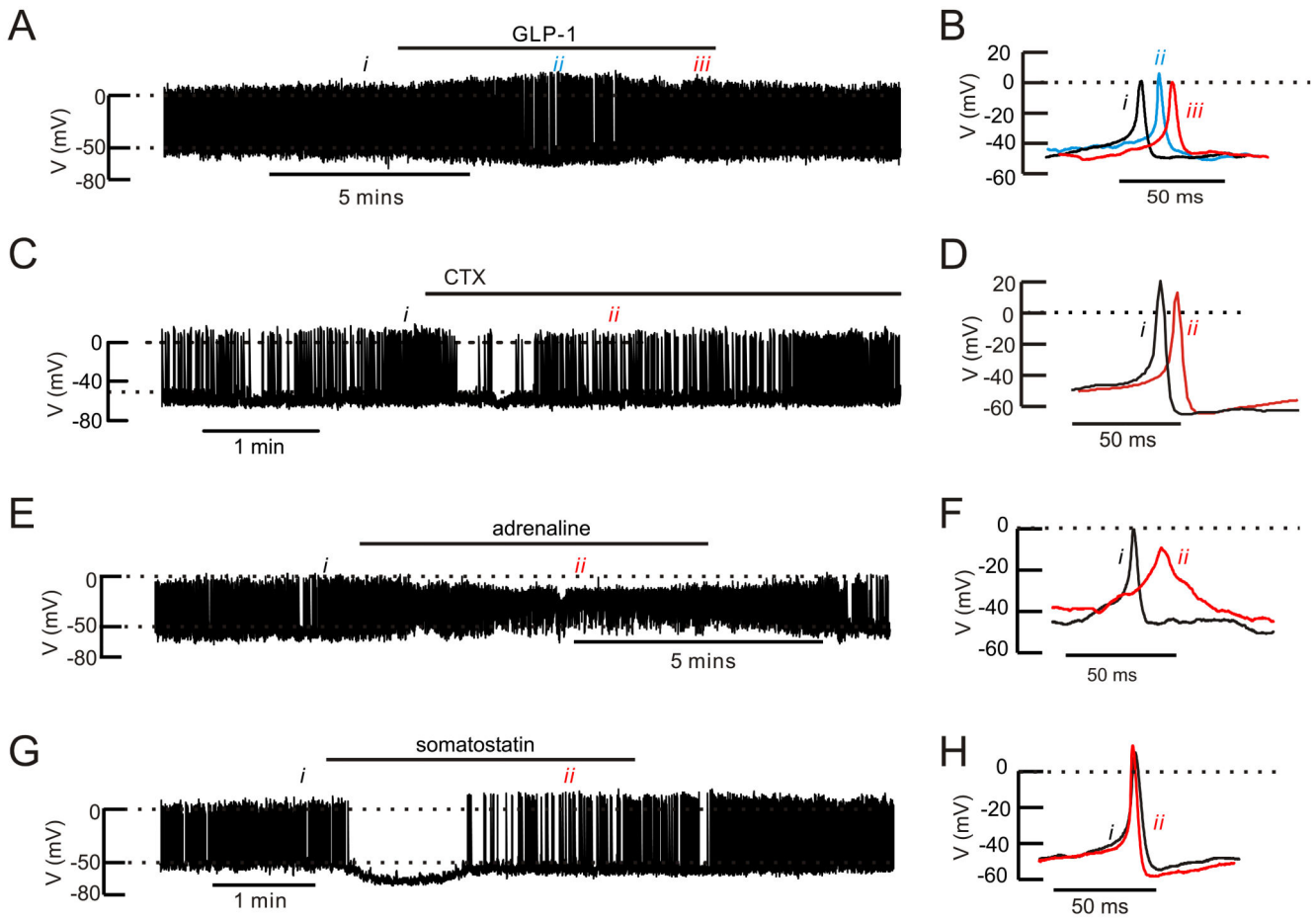

Figure 6.

Effects of GLP-1, ω-conotoxin, adrenaline and somatostatin on mouse α-cell electrical activity

(A) Action potential firing in an α-cell in an intact mouse islet at 1 mM glucose before, during and after addition of 10 nM GLP-1 (horizontal line).

(B) Examples of action potentials taken under control conditions (i), during the transient repolarization (ii) and at “steady-state” at the end of the GLP-1 application (iii).

(C) As in A but testing the effects of 100 nM ω-conotoxin on an isolated α-cell.

(D) Examples of action potentials recorded before (i) and after addition of ω-conotoxin (ii).

(E) As in A but 5 μM adrenaline was applied.

(F) Examples of action potentials under control conditions (i) and broad action potentials seen in the presence of adrenaline (ii)

(G) As in A but testing the effects of 100 nM somatostatin.

(H) Action potential recorded under control conditions (i) and when electrical activity had resumed in the continued presence of somatostatin (ii)

In A,C, E and F, the dotted horizontal lines indicate zero mV (top) and −50 mV (lower).

Europe PMC Funders Author Manuscripts

Europe PMC Funders Author Manuscripts

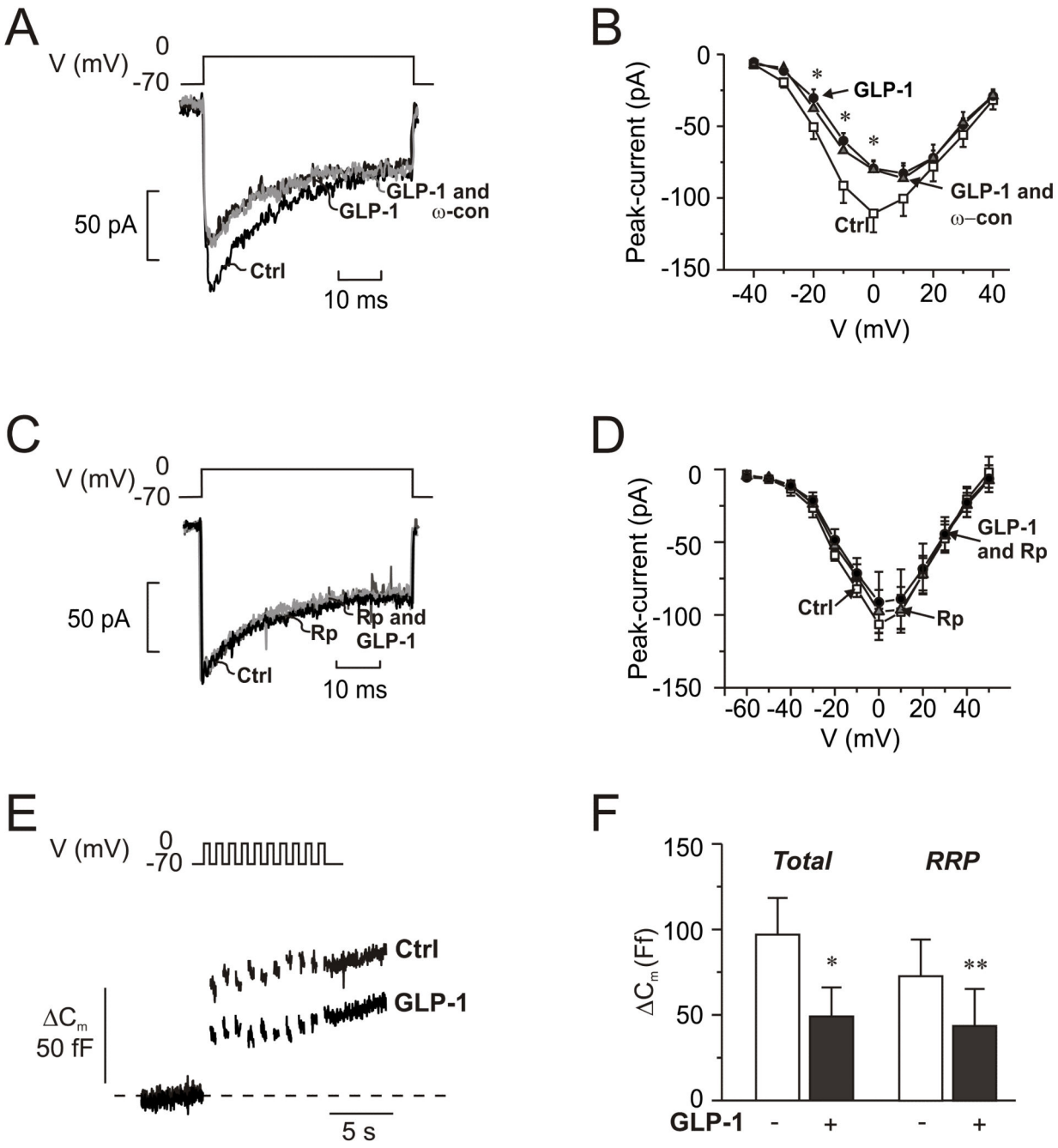

Fig. 7.

GLP-1 blocks N-type Ca^{2+}-channels and inhibits exocytosis.

(A) Whole-cell Ca^{2+}-currents evoked by membrane depolarization from −70 mV to 0 mV under control conditions (Ctrl; 1 mM glucose), 5 min after addition of GLP-1 (10 nM) and 5 min after addition of 100 nM ω-conotoxin in the continued presence of GLP-1 (GLP-1 and ω-con; grey).

(B) Current (I)-voltage (V) relationship recorded using the perforated patch whole-cell configuration under control conditions (□; n=10), 5 min after addition of 10 nM GLP-1 (●;

n=10), and 5 min after addition of ω-conotoxin (100 nM: ω-con) in the continued presence of GLP-1 (▲; n=6). *p<0.05 for effects of GLP-1 *vs.* control.

(C-D) As in A-B but recorded under control conditions (Ctrl, black), 6 min after the addition of 10 μM 8-Br-Rp-cAMPS (Rp; dark grey) and 4 min after addition of 100 nM GLP-1 in the continued presence of 8-Br-Rp-cAMPS (Rp and GLP-1; light gray) in α-cells

(E) Changes in membrane capacitance (ΔC_m) elicited by ten voltage-clamp depolarizations from −70 mV to 0 mV under control conditions (1 mM glucose; □), after the addition of 10 μM 8-Br-Rp-cAMPS (▲) and in the simultaneous presence of 10 nM GLP-1 8-Br-Rp-cAMPS (●).

(F) Histogram of the mean increase in membrane capacitance elicited by the entire train (Total) and increase evoked by the two first depolarizations (RRP). n=6; *p<0.05, **p<0.01.

Europe PMC Funders Author Manuscripts